Open Heterogeneous Data for Condition Monitoring of Multi Faults in Rotating Machines Used in Different Operating Conditions

Moncef Soualhi[1], Abdenour Soualhi[2], Khanh T. P. Nguyen[3], Kamal Medjaher[4], Guy Clerc[5] and Hubert Razik[6]

[1] *Université de Franche-Comté, SUPMICROTECH, CNRS, institut FEMTO-ST, F-25000 Besançon, France*
moncef.soualhi@univ-fcomte.fr

[2] *Laboratoire LASPI, University Lyon, UJM-Saint Etienne, 42100 Saint-Etienne, France*
abdenour.soualhi@univ-st-etienne.fr

[3,4] *Laboratoire Génie de Production, INP-ENIT, Université de Toulouse, Tarbes, 65000, France*
thi-phuong-khanh.nguyen@enit.fr
kamal.medjaher@enit.fr

[5,6] *University Lyon, Université Claude Bernard Lyon 1, INSA Lyon, École Centrale de Lyon CNRS, Ampère, UMR5005, 69622 Villeurbanne, France*
guy.clerc@univ-lyon1.fr
hubert.razik@univ-lyon1.fr

ABSTRACT

Rotating machines are widely used in several fields such as railways, renewable energies, robotics, etc. This diversity of application implies a large variety of faults of critical components susceptible to fail. For this purpose, prognostics and health management (PHM) is deployed to effectively monitor these components through the detection, diagnostics as well as prognostics of faults. In the literature, there exist numerous methods to ensure the above monitoring activities. However, few of them consider different failure types using heterogeneous data and various operating conditions. Also, there are no dominant methods that can be generalized for monitoring. For this reason, the genericity of these methods and their applicability in several systems is a crucial issue. To help researchers to achieve the above challenges, this paper presents a detailed description of data sources from experimental test benches. These data sets correspond to different case studies that monitor the health states of multiple critical components in various operating conditions using numerous sensors.

Keywords: Prognostics and health management, Condition monitoring, Open data science, Data processing, Health indicator, Fault detection and diagnostics, Electrical machines, Rotating machines, Mechanical faults, Electrical faults.

https://doi.org/10.36001/IJPHM.2023.v14i2.3497

1. INTRODUCTION

Nowadays, rotating machines are used in different applications such as transport, energy production, robotics, and the manufacturing industry (Lee et al., 2015; M. Soualhi, Nguyen, & Medjaher, 2020; Shi et al., 2022). Depending on the area of application of these machines, they undergo several types of failures (Kim et al., 2017). In fact, a rotating machine is the seat of dynamic forces of mechanical origin generated by moving parts. For example, an imbalance in the rotating shaft can cause an imbalance fault (sinusoidal excitation) (Lee et al., 2014), and chipping on a ball bearing track can lead to a shock (impulse excitation) when each ball passes over the fault (Ali et al., 2015). These forces cause vibrations as well as modifications in the signature of certain physical parameters. These parameters are measured by sensors and the obtained data are used to monitor the machine. Among them, one can cite current, voltage, force, vibration, temperature, speed, torque, and force. These measurements are injected into monitoring algorithms such as Prognostics and Health Management (PHM) to reveal the health state of the machine through the extraction of useful information named Health Indicators (HI) (Wang et al., 2017; A. Soualhi et al., 2014). The relevance of these indicators depends essentially on the position of the sensor and the surrounding noise, the availability and quality of data, and the operating conditions of the machine (Liu et al., 2015; Cuguero-Escofet et al., 2017; Gougam et al., 2019). Furthermore, the fault indicators of a component (bearing, motor, gear, belt, etc.) depend also on several fac-

tors such as the rotation speed, the load or the composition of the rotating machine (Adel et al., 2022). All of these factors can negatively impact the quality of the HI by generating false alarms (de Jonge et al., 2017).

To remedy this problem, some research works focused on the implementation of effective maintenance strategies based on reliable and automated fault detection, diagnostic, and prognostic algorithms (Souahli & Razik, 2020a,b). These strategies are Condition-Based Maintenance (CBM) and Predictive Maintenance (PM) (Chiachío et al., 2015; Strangas et al., 2021). In CBM, the interventions are executed depending on the current health state of the machine which can be observed on the HI (Kim et al., 2017; Benaggoune et al., 2022). When the HI of the machine reaches a defined threshold (critical state), the risk is considered significant and a maintenance action is scheduled (Caballé et al., 2015). In general, the threshold can be defined by standards or by experts throughout empirical experiments analysis (M. Soualhi, Nguyen, et al., 2022). Hence, CBM offers then the possibility of scheduling maintenance actions only when the machine's health state is considered out of nominal requirements, reducing therefore unnecessary replacements. In PM, the evolution of the HI is tracked in time to predict when they reach the failure threshold and to estimate the Remaining Useful Life (RUL) before the machine fails (Tamssaouet et al., 2021; Gougam et al., 2020). In this case, the maintenance interventions are then scheduled earlier based on the estimated RUL (de Pater & Mitici, 2021; Gouriveau et al., 2016). PM differs then from CBM by the prediction action of the HI, passing from the observed actual health state to the predicted health state.

However, in both maintenance strategies, experimental data are required to validate the models and the algorithms developed by PHM researchers and industrial practitioners. In this context, the experimental data can come from different sources, such as laboratory tests, field tests, or numerical simulations in order to create a benchmark data set (Sinha & Elbhbah, 2013). A benchmark data set is a set of physical measurements used to evaluate and compare the performance of PHM algorithms. Having good benchmark data sets is important for the following reasons:

- Performance evaluation: A well-designed benchmarking data set allows objective evaluation of the performance of different PHM algorithms and methods;
- Comparison: Good benchmark data sets makes it possible to compare the results of different algorithms and methods, which helps identify their strengths and weaknesses;
- Repeatability: Having a standard benchmark data set enables researchers and practitioners to reproduce and validate the results of others, which is essential for the development and improvement of data-driven PHM methods;

Benchmark data sets are therefore necessary to assess the performance of maintenance tasks Ramasso & Saxena (2014); H. Zhang et al. (2022). Indeed, industrial companies need hard evidence that the technologies offered can detect current abnormalities, predict future failures, and help plan maintenance interventions (Ramasso & Saxena, 2014). Experimental data are often expensive and difficult to obtain, so it is important to ensure that they are relevant and reliable. Poor quality data can lead to erroneous conclusions or inaccurate predictions, which can have costly and potentially dangerous consequences, especially in industries where safety is a significant concern, such as nuclear, aerospace, energy, and transportation. The creation of a benchmark data set involves case studies implementing different types of faults to enable researchers to test their models and algorithms (Vachtsevanos et al., 2006; Goel et al., 2022). These data can be exploited to know the real conditions under which the faults occur and to measure their impact on the performance of the machine. The defects can include mechanical failures, electronic failures, fluid leakages, disruptions in manufacturing processes, etc (Saxena, Goebel, et al., 2008; M. Soualhi, Nguyen, & Medjaher, 2020). The data can also be used to train and test fault detection, diagnostic and prognostic methods to improve their accuracy, robustness, and repeatability (L. Zhang et al., 2019). In addition, these data are also important to assess the effectiveness of maintenance strategies. They can be exploited to evaluate the impact of the interventions on the machine lifespan, its availability, and the maintenance costs (Campbell et al., 2016).

To ensure the good quality of a benchmark data set, it is important to clearly define the objectives of the case study and plan the experiments accordingly. It is also important to have quality control procedures to ensure the reliability and validity of the data Omri et al. (2021). This may include the use of accurate and repeatable measurement techniques, standardized protocols for sampling and data analysis, and cross-validation testing to verify data consistency Sant'Ana et al. (2016). Additionally, it is important to collect data over a long enough period of time to allow meaningful statistical analysis and to ensure that the environmental and operational conditions are varied enough to cover a range of fault scenarios (Kibria et al., 2018).

In conclusion, good benchmark data sets play a crucial role in advancing the field of data-driven methods for fault diagnosis and prognosis Nguyen et al. (2022). They provide a common standard for the evaluation, comparison, and improvement of algorithms and systems.

Therefore, this paper contributes to the development of PHM research and the dissemination of more reliable and accurate results for different rotating machinery applications in the industry. It provides in Section 2 a comprehensive review of existing data sets for PHM, highlighting both the advantages

and limitations of these data sets. Then, it presents in Section 3 new reliable benchmark data sets for researchers and practitioners to develop and evaluate PHM solutions. It also provides valuable information on the experimental settings used to collect the data. By using this information as a guide, industrial practitioners can build their own test benches for their specific case studies. Finally, preliminary works conducted with these new data sets are summarized. These will serve as a resource for future researchers to explore the different developments, data used and compare their own results and improve their own PHM approaches.

2. EXISTING BENCHMARK DATA SETS FOR PHM OF ROTATING MACHINE IN INDUSTRY

As mentioned in the previous section, benchmark data sets are essential to develop and evaluate PHM techniques. These data sets provide a standardized platform for researchers to compare and improve their algorithms, making it easier to identify the most effective and accurate tools and methods. Table 1 summarizes several widely used benchmark data sets for PHM of the rotating machine applications in industry, including the Bearing Data Center at Case Western Reserve University (CWRU), the NASA Prognostics Center of Excellence, and the IMS Center at the University of Cincinnati. These data sets contain information about various types of rotating machines, such as motors, generators, and turbines. As shown in Table 1, the majority of the benchmark data sets are primarily concerned with bearing faults. It is worth noting that the dominance of literature on bearing faults in PHM may be attributed to the importance of bearings as critical components in various industrial systems. Among these data sets, the CWRU, MFPT, and Paderborn University data sets investigate different types of bearing faults, whereas the FEMTO-ST, XJTU-SY, and IMS data sets consider the bearing degradation process during accelerated tests. Besides, researchers can leverage the CWRU and FEMTO-ST data sets to develop algorithms that account for the impacts of different operating conditions, such as variations in load and speed. Along with the bearing faults, several other fault types of rotating machines in the industry have been investigated. For example is the data sets of milling machines (NASA Milling data set and PHM10-CNC Milling machines), which consist of measurements from the milling machine performing various cutting operations. These data sets are used to develop algorithms for tool wear monitoring and prediction, a critical aspect of CNC machining operations. They provide researchers with valuable resources to evaluate the effectiveness of the proposed condition monitoring and prognostics methods for applications in industrial manufacturing and machining processes. Another significant application area of PHM is aircraft engines, where crucial components like turbofan engines must be continuously monitored to detect, diagnose, and predict their potential faults to ensure safe and reliable operation. Several benchmark data sets are available for researchers to develop and evaluate PHM methods for turbofan engines. One such data set is the CMPAPSS-2008 data set, which includes measurements from different turbofan engines under different combinations of operating conditions and fault modes. Similarly, the PHM-2008 data set was provided for the data challenge held at the 1st International Conference on Prognostics and Health Management (PHM08). One of the significant advantages of these data sets is their diverse range of sensors that provide different types of measurements. This diversity enables researchers to choose the relevant measurements for their specific PHM algorithms and filter out irrelevant or noisy data. Furthermore, the heterogeneity of the data sets presents an opportunity for researchers to develop approaches for handling heterogeneous data sources. Although the diversity and heterogeneity make CMAPSS-2008 and PHM-2008 become valuable resources for PHM researchers to develop and test their algorithms for applications where data may come from different sensors or sources, they are simulation-based data and thus may not accurately reflect real-world conditions. To overcome this drawback, the CMAPSS-2021 data set has been recently introduced. It provides synthetic run-to-failure degradation trajectories for nine turbofan engines with different initial health conditions. The engines were subjected to real flight conditions, which were recorded onboard a commercial jet, and these data were used as input to the C-MAPSS model. This data set enables researchers to develop and evaluate PHM methods for a range of faults and real-world operating conditions, which can be challenging to capture through experimentation alone. However, similar to CMAPSS-2008 and PHM-2008 data sets, one of its significant limitations is the anonymization of the data. This means that no information about the sensors used or the sampling frequency is available. This lack of information can be problematic for researchers and practitioners who want to integrate aero-domain knowledge into their machine-learning models. Additionally, the absence of sensor information and sampling frequency can make it challenging to interpret the results of the PHM algorithms, as the data may be noisy or irrelevant.

To provide data for other industrial applications, the International Conferences on PHM organized data challenges in 2011, 2018, and 2021 providing data for other industrial applications, such as the detection of cup anemometer faults, diagnostics and prognostics of ion mill etching system faults, and diagnostics of rock drill machine faults. These data can help researchers developing and testing their algorithms in different applications, contributing to the advancement of PHM in various application domains. However, the major limitation of these data sets is the lack of detailed experimental settings. Therefore, without these informations, it becomes difficult to design algorithms that consider the specific operating conditions of the machines.

Table 1. Open Benchmark data sets.

data set	Main objectives	Characteristics
CWRU data set (click here)	Diagnostics of bearing faults	**Vibration signals**. 16-channel digital audio tape recorder for data acquisition. Sampling frequency of 12kHz and 48kHz. Motor loads from 0 to 3 horsepower, with motor speeds of 1720 to 1797rpm.
Paderborn University data set (click here)	Diagnostics of bearing faults	**Synchronously measured motor currents and vibration signals** (high resolution). Sampling frequency of 64kHz. Supportive measurement of speed, torque, radial load, and temperature. Four different operating conditions. 20 measurements of 4 seconds each for each settings.
FEMTO-ST data set (click here)	Prognostics of bearing faults	**Temperature and vibration signals**. Vibration signals were recorded every 10 seconds with sampling frequency 25.6kHz. 17 run-to-failure data under three different operating conditions, but unknown faulty mode of the failed bearing under each test, Nectoux et al. (2012).
MFPT data set (click here)	Diagnostics and prognostics of bearing faults	**Data (vibration signals)** from a bearing test rig: nominal bearing data, outer and inner race faults at various loads (0–1334 N bearing load), and three real-world fault. Input shaft rate of 25Hz. Baseline conditions: sample rate of 97,656 samples per second (sps), for 6 seconds. Faulty conditions: sample rate of 48,828 sps, for 3 seconds.
IMS data set (click here)	Prognostics of bearing faults	**Vibration signals**: 1-second recorded at specific intervals. Sampling rate of 20kHz. Run-to-failure data. 4 test bearings mounted on one shaft driven by an AC motor and coupled by rub belt. Motor speed of 2000rpm.
XJTU-SY Bearing data set (click here)	Prognostics of bearing faults	**Vibration signals** (horizontal and vertical accelerometers). Sampling rate of 25.6kHz for 1.28 seconds of every minute. Run-to-failure data of 5 bearings LDK UER204. 3 different operating conditions (different rotating speeds and radial force).

NASA Milling data set (click here)	Prognostics of milling tool's faults	**Acoustic emissions, vibrations and current signals**. Sampling rate of 250Hz. Run-to-failure data of sixteen milling tools of MC-510V milling center. 8 different operating conditions (different depth of cut, feed rate and material).
PHM10-CNC Milling machines (click here)	Prognostics of high-speed milling machine's fault	**Dynamometer, accelerometer, and acoustic emission data.** Six individual cutter records. The spindle speed of the cutter was 10400rpm; feed rate was 1555 mm/min; Y depth of cut (radial) was 0.125 mm; Z depth of cut (axial) was 0.2 mm. Data were acquired at 50kHz/channel.
CMAPSS-2008 (click here)	Prognostics of turbofan engines faults	**Multivariate time series (21 sensors)** from different engines. Each engine starts with different degrees of initial wear and manufacturing variation and works under three operational settings. No information about the sampling frequency.
PHM-2008 (click here)	Prognostics of turbofan engines faults	**Similar to the one posted above**. Data challenge competition held at the international conference PHM08. The true Remaining Useful Life (RUL) values are not revealed.
CMAPSS-2021 (click here)	Prognostics of turbofan engines' faults	**Similar to CMAPSS-2008.** New realistic data set of run-to-failure trajectories for a small fleet of aircraft engines under realistic flight conditions.
PHM11 Data Challenge (click here)	Detection of cup Anemometer's fault	**Anemometers, a weather vane, and a temperature sensor**. Each sensor measures data over a 10-minute period and reports the average, standard deviation, minimum and maximum value over that 10-minute period.
PHM18 Data Challenge (click here)	Diagnostics and Prognostics of Ion Mill Etching System's fault	**Multivariate time series (5 sensors)**. No information about sampling frequency. The system works under different operating settings. Three different failure modes of interest: flow cool pressure dropped below the limit, flow cool pressure too high check flow cool pump, and flow cool leak.
PHM21 Data Challenge (click here)	Diagnostics of rock drill machine's fault	**Pressure sensor data**. No information about the sampling frequency. The training data set contains data from 10 different failure modes and one healthy class.

Overall, while the data sets presented in Table 1 offer valuable resources for PHM research, it is essential to consider their limitations and drawbacks to ensure that the algorithms developed using these data sets can be effectively applied to real-world industrial applications. One of their major limits is, despite the industrial practitioners appreciate the importance of PHM of rotating machines, and due to the data security issue, almost studies in literature use data from laboratory test benches. Additionally, it is worth noting the lack of diversity in the fault types and the operating conditions of these data sets Magnus & Jing (2019). For instance, those on bearings focus primarily on bearing faults, which limits their applicability to other types of components or systems. Hence, the study of combined faults and their severity is still rare. This can also hinder the applicability of the developed algorithms under practical settings, where combined faults and operating conditions may arise. Moreover, one can notice that the availability of abundant information obtained through high sampling rates has proved crucial for effective fault detection and diagnosis of rotating machines, particularly in the context of vibration data analysis. Several works exploit frequencies between 20kHz and 64kHz for efficient information extraction on system health, we can cite Jiang et al. (2022) which propose 20kHz for gear and bearing monitoring, while in Zarei et al. (2014); Golafshan & Sanliturk (2016) the authors propose 32kHz for bearing monitoring, and 50kHz for gear monitoring in Ooijevaar et al. (2019). In Chen et al. (2018), the sampling frequency is fixed 64kHz for bearing monitoring. However, the application of these sampling rates to the analysis of other types of data, such as current, voltage or other relevant parameters, is relatively less investigated. Therefore, the development of data sets covering a wider range of faults and operating conditions with high sampling rates across multiple data types can aid tin the advancement of PHM research and the practical implementation of PHM algorithms.

3. DESCRIPTION OF NEW BENCHMARK DATA SETS

In this section, different data sets (DATA-PHM) of test benches used for monitoring multiple faults in rotating machines are presented. The presentation of these test benches is classified into two categories: 1) test benches for the monitoring of rotating motors and 2) test benches for monitoring the systems connected to the motor.

First, subsection 3.1 presents a data set on monitoring of motor rotor faults while subsection 3.2 presents monitoring data of motor stator faults. Then, a data set related to the health monitoring of bearings and gears of a gearbox connected to a motor is presented in subsection 3.3. After that, monitoring data of a machining tool placed at a spindle motor in a multi-axis robot are described in subsection 3.4 while a data set on rotating shaft monitoring of each robot axis is presented in subsection 3.5. Finally, subsection 3.6 is dedicated for summarizing the proposed data sets as well as the publications using these data sets.

3.1. AMPERE data set: detection and diagnostics of motor rotor faults

The AMPERE laboratory test bench is designed to monitor two parts, 1) monitor the rotor of the motor and 2) monitor the stator of the motor. Hence, there are two sets of data corresponding to the two different monitoring cases mentioned above. The first data set concerns the monitoring of the electrical bars and the bearing at the rotor level with data from the inverter output. The second data set corresponds to the monitoring of the motor stator windings with data collected from the power grid.

This test bench is composed of a three-phase inverter to supply and control a 5.5kW electric motor (see Table 2). The motor used is a squirrel cage motor and its rotating shaft is connected to an electromagnetic brake which operates as a load on the motor. This brake, achieved at a nominal speed, is designed to dissipate a maximum power of 5kW with a maximum brake torque of 100N.m. The overall view of the test bench is shown in the Appendix section.

Table 2. Characteristics of the AMPERE test bench motor.

Characteristic parameters	Value
Protection class (IP)	55
Normalized operating temperature	40°C
Nominal voltage between phases	400V
Power supply frequency	50Hz
Nominal speed	1440rpm
Nominal power output	5.5kW
Power factor	0.84
Nominal current	11.4A
Number of pole pairs (p)	2
Stator resistance per phase	1.315 Ω
Number of rotor slots (Nr)	28
The number of slots on the stator (Ns)	48

The whole test bench is equipped with several heterogeneous sensors placed at different positions. There are three-phase current and voltage sensors corresponding to the three phases of the motor. Furthermore, three separate accelerometers are placed on the motor. The first one is in the vertical direction on the opposite side of the coupling. The second one is in a parallel direction to the motor axis on the opposite side of the coupling. The last one is in a horizontal direction and perpendicular to the motor axis on the opposite side of the coupling. Finally, an encoder placed at the output of the brake is used to measure the rotation speed. The acquisition system, Odyssey Gould Nicolet, used to measure these signals has eight differential inputs, known as fast channels, which can be sampled at up to 10MHz on 14 bits. These inputs were used

to measure the voltages as well as the currents. In addition, there are eight common mode inputs, called slow channels, on which the sampling frequency can reach 1M on 16 bits. One of these eight inputs was used to measure the rotation speed. Then, three inputs are reserved for accelerometers to measure the vibration. Figure 1 shows a scheme of the test bench that highlights the different connections and sensors mentioned above.

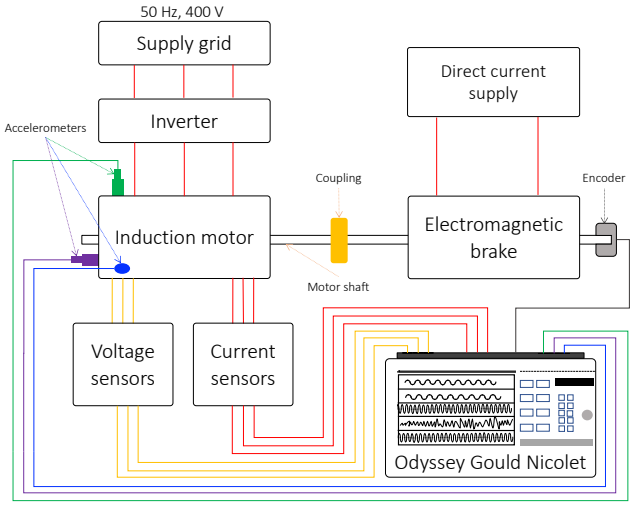

Figure 1. AMPERE test bench scheme.

All acquisitions are performed in the permanent mode over a period of 5 seconds with a sampling frequency of 20kHz. The data are stored in .mat and .csv files with 11 columns. Column 1 represents the time steps (t) acquisition. Columns 2 to 4 represent the three-phase voltage signals (V_a, V_b, V_c). Columns 5 to 7 are the three-phase current signals (I_a, I_b, I_c). Column 8 is the speed (S) while the last three columns, from columns 9 to 11, are for the three accelerometers (Acc_a, Acc_y, Acc_z).

Regarding the monitoring data set of the electrical bars and the motor bearing, 25 experiments are carried out with data collected at the output of the inverter. In detail, there are 5 different experiments (health states) of the motor, a healthy state with a healthy rotor, breakage of one rotor bar, breakage of three rotor bars, breakages of four rotor bars, and a degraded bearing. The broken rotor bars was made by creating holes in bar conductors, 1 hole for 1 broken bar, 3 holes for 3 broken bars, and so on. Regarding the bearing degradation, the damage is caused when an electric current flows through the bearing, i.e. from one ring to another via the rolling elements. In each health state, 5 operating conditions which are load levels (0%, 25%, 50%, 75% and 100%) representing the resistant torque generated by the brake, were applied separately in each experiment.

To calculate the numerical torque value, we can estimate the numerical value of the load level on the basis of the motor's nominal values. In this test bench, the nominal motor data is a power of 5.5kW with a speed of 1440rpm, therefore the 100% load level of this motor is a resistant torque equal to 32N.m. The remaining load level values can be deduced using the proportion method. The overall experiment details are summarized in Appendix, Table 5.

3.2. AMPERE data set: detection and diagnostics of motor stator faults

As mentioned in the above subsection, there are two data sets corresponding to two different condition monitoring studies. In this subsection, the data from the power grid supply for monitoring the stator behavior is studied In this case, different resistances are added to one of the stator windings in order to reproduce a short circuit between the windings of the b-phase of the motor and cause an unbalance supply. Besides, the composition of the test bench remains unchanged from what has been described in subsection 3.1. Also, the data collection procedure remains the same, i.e. the sampling frequency is equal to 20kHz with an acquisition period/file of 5 seconds in .mat files. In these files, column 1 represents the acquisition time (t). Columns 2 to 4 represent the voltage measurements (V_a, V_b, V_c). Columns 5 to 7 contain the signals of the three-phase currents (I_a, I_b, I_c). Column 8 is for the instantaneous motor rotation speed (S) while columns 9 to 11 are for the accelerometers (Acc_x, Acc_y, Acc_z).

In total, 25 experiments were performed for monitoring the stator power supply with data collected from the supply grid. There are 5 different health states of the motor: a healthy state of the stator and four states representing different unbalanced supply levels of 5%, 10%, 20%, and 40%. In each health state, 5 load levels, 0%, 25%, 50%, 75%, and 100% generated by the brake were applied separately for each health state. Here, similarly to rotor fault conditions, the 100% load level is equal to 32N.m. The overall experiment details are summarized in Appendix, Table 6.

3.3. LASPI data set: detection and diagnostics of bearing, gear and combined faults of gearbox

The LASPI test bench is used for monitoring the bearing and gear faults of a gearbox. It is composed of a three-phase inverter to supply and control a three-phase induction motor of 1.5kW. This latter motor drives a gearbox on which the components of the study are positioned. Also, there is an electromagnetic brake connected to the gearbox. This latter component is used to simulate a load on the motor. The motor characteristics are presented in Table 3, and the overall view of the test bench is shown in Appendix, Figure 6. In detail, the gearbox has three shafts, the input shaft, the intermediate shaft, and the output shaft. The studied components are placed in the intermediate shaft as shown in the diagram

of Figure 6. The input shaft, which is directly connected to the rotating shaft of the motor, has one gear and two bearings installed on each side of the gearbox.

Table 3. Characteristics of the LASPI test bench motor.

Characteristic parameters	Value
Protection class (IP)	43
Normalized operating temperature	40°C
Nominal voltage between phases	380V
Power supply frequency	50Hz
Nominal speed	2850rpm
Nominal power output	1.5kW
Power factor	0.80
Nominal current	11.4A

The gear is installed at the brake side and contains 29 teeth. The two bearings contain 9 rolling balls with a diameter of 0.3125 inches, a pitch diameter of 1.5157 inches, and a contact angle equal to 0.

Besides, the intermediate shaft has two bearings, with the same characteristics as the ones of the input shaft, and two gears. The first gear installed on the motor side has 36 teeth while the gear installed in the brake side has 100 teeth. Finally, the output shaft which is directly connected to the electromagnetic brake has the same bearings as the previous ones and a gear installed on the motor side with 90 teeth.

This test bench is equipped with different sensors and an acquisition system to collect the monitoring data. It has three current and voltage sensors, placed at the output of the inverter that supplies the motor, and an accelerometer placed as near as possible to the studied components of the intermediate shaft. The data acquisition is performed by National Instrument 9234 cards. The overall scheme of the test bench is given in Figure 2.

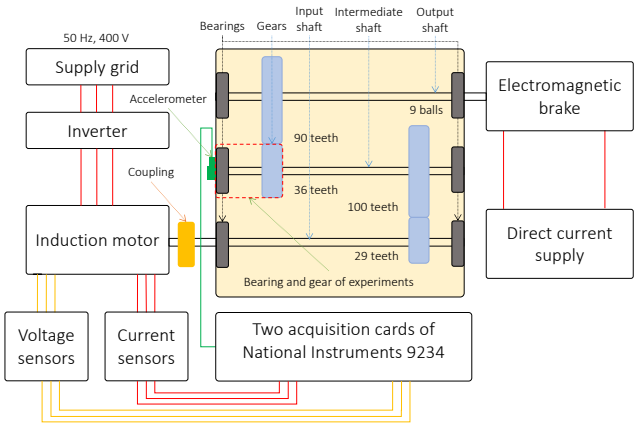

Figure 2. LASPI test bench scheme.

All acquisitions are performed in the permanent mode over a period of 10 seconds with a sampling frequency of 25.6 kHz. The data are stored in .csv files with 7 columns. Columns 1 to 3 represent the three-phase current signals (I_a, I_b, I_c) with a reduced gain of 100. Column 4 represents the vibration signal (Acc) with a sensitivity of 100 mV/g. The last columns, from 5 to 7, represent the voltage signals of the three phases (V_a, V_b, V_c) with a reduction gain of 200. Based on the test bench instrumentation mentioned above, 84 experiments were conducted to monitor separately the bearing and the gear faults, as well as their combination. In detail, 7 health states are studied: healthy states of the bearing and the gear, a gear surface fault, a gear half-tooth breakage fault, a bearing inner ring fault, a bearing outer ring fault, combined faults between the gear surface fault and the bearing inner ring fault, and finally combined faults between the gear half-tooth breakage fault and the bearing outer ring fault. Note that the LASPI case study is a didactic platform that is delivered with components that already contain a defect, so that only the original component needs to be replaced by the damaged one. In addition to these health states, each state is tested under three different rotating speeds separately, 1500rpm, 2100rpm, and 2700rpm, and at each speed four load levels, 0%, 25%, 50%, and 75%, are also performed separately. To obtain the load level value at the 75%, it is necessary to first calculate the load value at 100% using the nominal motor characteristics, i.e. 1.5kW power and 2850rpm, producing a resistant torque of 5N.m. Then, the proportion method can be utilized to deduce the load at the 75% level and the remaining ones. The experiment details are summarized in Appendix, Table 7.

3.4. METALLICADOUR robot-tool data set

The test bench of METALLICADOUR Technology Transfer Center is designed for two purposes: 1) monitoring the health state of a machining tool mounted on the motor spindle at the end of the robot axis and 2) monitoring drifts of the robot axes. In this subsection, the data set related to the monitoring of the machining tools is presented. The robot in use is an ABB 6660 having six axes of rotation (6 arms), each axis being an alternative servo-motor. A three-phase motor carrying the machining tool is mounted at the end of the sixth axis. The cutting tool is used for machining aluminum pieces and contains three cutting edges. Regarding the manufacturing piece, it consists of a small aluminum part used in aeronautic industry. Behind the robot, an IRC5 controller is used to power and control its axes. An inverter is also used to power the machining spindle. An overview of the test bench is shown in Appendix, in Figure 7.

This test bench is equipped with different types of sensors. Three current sensors are placed at the output of the inverter, and correspond to each phase of the tool spindle. On the flange of the machining spindle, as close as possible to the machining unit, a three-axis accelerometer (x-axis, y-axis,

and z-axis) is also placed. Finally, a three-axis force and torque sensor is installed between the sixth axis of the robot and the machining spindle. The motor characteristics and test bench scheme are presented in Table 4 Figure 3, respectively.

Table 4. Characteristics of the METALLICADOUR test bench spindle motor.

Characteristic parameters	Value
Nominal voltage between phases	380V
Power supply frequency	50Hz
Nominal speed	18000rpm
Nominal power output	44kW
Power factor	0.84
Nominal current	22A
Number of pole pairs (p)	2

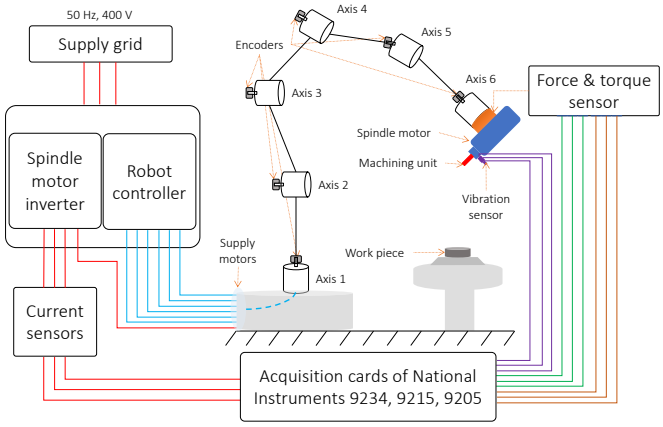

Figure 3. METALLICADOUR test bench scheme.

The monitoring data are collected over a period of 5 seconds with a sampling frequency equal to 25.6kHz and are stored in .csv files with 12 columns. Columns 1 to 3 represent the three-phase current signals (I_a, I_b, I_c), columns 4 to 6 correspond to the three-axis force signals (F_x, F_x, F_z), columns 7 to 9 are for the three-axis torque signals (T_x, T_y, T_z), and columns 10 to 12 are for the three-axis accelerometer (Acc_x, Acc_y, Acc_z).

Concerning the tool monitoring, 16 experiments were performed to collect the data. In total, 4 tool states were studied: a healthy state of the tool, a tool surface damage, a tool flack damage, and a tool broken tooth. The three faulty tools are three different tools already used for machining aluminum parts. After each machining operation, a 3D measuring system called ALICONA, which reconstructs the image of the tool edge, was used to quantify with experts the state of the tool (defect 1, defect 2, etc.). For example, a tool was used for 6 machining operations before the experts, with the help of the ALICONA imaging system, determined that the tool had reached a first level of degradation. In each health state, 4 operating condition were investigated separately by varying 3 parameters separately: cutting depth, spindle speed and spindle feed rate. The conducted experiments are summarized in Table 8.

3.5. METALLICADOUR robot-axes data set

As mentioned in the previous subsection, this data set is dedicated to the monitoring of robot axes drifts where the motion of each axis is performed by an alternating current servomotor. However, in this application, the robot is used for machining aluminum parts, consisting of a labyrinth shape aiming to move all the robot axes, which is a different shape than the previous one (see Figure 8).

The previously installed sensors (current, force, torque and vibration) related to the machining tool are still valid. However, new data related to the displacement of each axis are additionally collected in this study. They are the position data from the encoders placed on the rotating shaft of each axis.

The data set related to robot tool sensors are collected over a period of 5 seconds with a sampling frequency of 25.6kHz in .csv files with 12 columns, while the position data of each axis of the robot are collected with a sampling frequency of 41.6Hz in .xlsx files with 9 columns. The 12 columns of the tool data are the three-phase current, the three-axis force, the three-axis torque and the three-axis vibration signals. In the .xlsx files, column 1 is the time step (t) acquisition, columns 2 to 7 are the position data from axis 1 to axis 6 (P_{a1}, P_{a2}, P_{a3}, P_{a4}, P_{a5}, P_{a6}) columns 8 to 10 are the x, y, and z coordinates of the tool center position (P_{tx}, P_{ty}, P_{tz}) relative to the object coordinates (user coordinates), and columns 11 and 12 are the index of the machining start time I_tm, and the index acquisition trigger I_ta, respectively. These last two parameters are equal to 0 or 1. Zero value in both cases means that the activity of the machining and acquisition has not yet started. Otherwise, one value means that the machining process has started and the acquisition has been initiated.

In total, 14 experiments were conducted. The first group of experiments contains one healthy state of the robot without any drifts (the reference case) and 6 experiments with single drifts on each axis. The second group of experiments contains another healthy state without drifts and 6 health states with combined drifts between the robot axes, e.g. drifts in both axis 4 and axis 6 simultaneously. These experiments are summarized in Appendix, Table 9.

3.6. Summary of related publications

The proposed data sets has been the subject of several works published in the literature. These works have mainly focused on the development of data processing methods for the con-

struction of health indicators and/or diagnostic tools based on classification algorithms. The common body of work suggests that the data set can be used to extract meaningful information, which allows the identification and proposal of new monitoring models. In addition, these studies have demonstrated the potential of the data set to improve diagnostic accuracy and enable more precise and customized management recommendations. A summary of these published works is presented in Appendix, Table 10. Moreover, future users and contributors who use these data sets will be able to exploit the obtained results from the works mentioned in Table 10 with the associated metrics to evaluate the performance of their new approaches. Note that contributors are free to use their own metric or already existing ones for the evaluation of their approaches (Saxena, Celaya, et al., 2008).

The data sets presented above in this paper are available on the web and have been grouped into a collection by the laboratory that generated them. The collection is accessible through the link below (DATA-PHM). Grouping these data sets into a single collection makes it easier for researchers to access all the data and perform their own monitoring algorithms. For those interested in accessing separately the data sets, we have provided the DOI link for each one. The first DOI link (DATA-AMPERE) is for the AMPERE laboratory, which provides data for stator and rotor monitoring of an electric motor. The second DOI link (DATA-LASPI) concerns the LASPI laboratory, it provides data for monitoring gearbox system. Finally, METTALICADOUR center provides data for monitoring multi-axis robot and are accecible through the third DOI link (DATA-METALLICADOUR).

4. CONCLUSION

This paper reviewed existing open benchmark data sets for Prognostics and Health Management (PHM) of rotating machines and presented newly developed ones. The review has shown that the existing open data sets have provided valuable resources for testing and evaluating the effectiveness of condition monitoring for fault detection, diagnostics, and prognostic methods. However, in this review, certain limitations associated with these data sets were identified. One such limitation is the lack of information about the experimental setting, which can discourage PHM practitioners who wish to replicate these experiments. Moreover, the existing data sets also lack diversity in terms of fault types and operating conditions. These limitations highlighted the need for new benchmark data sets that cover a wider range of fault types and operating conditions and provide comprehensive information about the experimental settings. This valuable information on the experimental settings can guide researchers and industrial practitioners in constructing their own test benches to collect data that are specific to their case studies.

In addition, the works already developed on the proposed data sets has led to significant progress in the data processing algorithms for fault detection and diagnostics. We have used these data to develop and test innovative PHM solutions with promising results. The availability of this public data set has facilitated collaboration and knowledge-sharing across the industry, leading to improved performance, efficiency, and sustainability of industrial operations. We believe that the continued use and exploration of these data will drive further innovation in the field and contribute to the development of more reliable and effective maintenance strategies. We encourage researchers and industries to exploit these data and other public data sets to enhance maintenance practices and ensure the longevity of industrial systems. Note that we are continuously updating our data collection with new information and data, and we welcome contributors who wish to share their ideas and new data with us for open access. If you would like to contribute to this project please feel free to contact the corresponding author by email.

REFERENCES

Adel, A., Hand, O., Fawzi, G., Walid, T., Chemseddine, R., & Djamel, B. (2022). Gear fault detection, identification and classification using mlp neural network. In *Recent advances in structural health monitoring and engineering structures: Select proceedings of shm and es 2022* (pp. 221–234). Springer.

Ali, J. B., Fnaiech, N., Saidi, L., Chebel-Morello, B., & Fnaiech, F. (2015). Application of empirical mode decomposition and artificial neural network for automatic bearing fault diagnosis based on vibration signals. *Applied Acoustics*, *89*, 16–27.

Benaggoune, K., Yue, M., Jemei, S., & Zerhouni, N. (2022). A data-driven method for multi-step-ahead prediction and long-term prognostics of proton exchange membrane fuel cell. *Applied Energy*, *313*, 118835. doi: https://doi.org/10.1016/j.apenergy.2022.118835

Breuneval, R., Clerc, G., Nahid-Mobarakeh, B., & Mansouri, B. (2018). Classification with automatic detection of unknown classes based on svm and fuzzy mbf: Application to motor diagnosis. *AIMS Electronics and Electrical Engineering*, *2*(3), 59–84.

Caballé, N. C., Castro, I. T., Pérez, C. J., & Lanza-Gutiérrez, J. M. (2015). A condition-based maintenance of a dependent degradation-threshold-shock model in a system with multiple degradation processes. *Reliability Engineering & System Safety*, *134*, 98–109.

Campbell, J. D., Jardine, A. K., & McGlynn, J. (2016). *Asset management excellence: optimizing equipment life-cycle decisions*. CRC Press.

Casimir, R., Boutleux, E., Clerc, G., & Yahoui, A. (2006). The use of features selection and nearest neighbors rule for

faults diagnostic in induction motors. *Engineering Applications of Artificial Intelligence*, *19*(2), 169–177.

Chen, Y., Peng, G., Xie, C., Zhang, W., Li, C., & Liu, S. (2018). Acdin: Bridging the gap between artificial and real bearing damages for bearing fault diagnosis. *Neurocomputing*, *294*, 61–71.

Chiachío, J., Chiachío, M., Sankararaman, S., Saxena, A., & Goebel, K. (2015). Condition-based prediction of time-dependent reliability in composites. *Reliability Engineering & System Safety*, *142*, 134–147.

Cuguero-Escofet, M. A., Puig, V., & Quevedo, J. (2017). Optimal pressure sensor placement and assessment for leak location using a relaxed isolation index: Application to the barcelona water network. *Control Engineering Practice*, *63*, 1–12.

de Jonge, B., Teunter, R., & Tinga, T. (2017). The influence of practical factors on the benefits of condition-based maintenance over time-based maintenance. *Reliability engineering & system safety*, *158*, 21–30.

de Pater, I., & Mitici, M. (2021). Predictive maintenance for multi-component systems of repairables with remaining-useful-life prognostics and a limited stock of spare components. *Reliability Engineering & System Safety*, *214*, 107761.

Goel, A. K., Singh, G., & Naikan, V. N. A. (2022). A methodology for selection of condition monitoring techniques for rotating machinery. *International Journal of Prognostics and Health Management*, *13*(2).

Golafshan, R., & Sanliturk, K. Y. (2016). Svd and hankel matrix based de-noising approach for ball bearing fault detection and its assessment using artificial faults. *Mechanical Systems and Signal Processing*, *70*, 36–50.

Gougam, F., Rahmoune, C., Benazzouz, D., & Merainani, B. (2019, sep). Bearing fault diagnosis based on feature extraction of empirical wavelet transform (EWT) and fuzzy logic system (FLS) under variable operating conditions. *Journal of Vibroengineering*, *21*(6), 1636–1650. Retrieved from https://doi.org/10.21595/jve.2019.20092 doi: 10.21595/jve.2019.20092

Gougam, F., Rahmoune, C., Benazzouz, D., Varnier, C., & Nicod, J.-M. (2020). Health monitoring approach of bearing : Application of adaptive neuro fuzzy inference system (anfis) for rul-estimation and autogram analysis for fault-localization. In *2020 prognostics and health management conference (phm-besançon)* (p. 200-206). doi: 10.1109/PHM-Besancon49106.2020.00040

Gouriveau, R., Medjaher, K., & Zerhouni, N. (2016). *From prognostics and health systems management to predictive maintenance 1: Monitoring and prognostics*. John Wiley & Sons.

Jiang, G., Jia, C., Nie, S., Wu, X., He, Q., & Xie, P. (2022). Multiview enhanced fault diagnosis for wind turbine gearbox bearings with fusion of vibration and current signals. *Measurement*, *196*, 111159.

Kibria, M. G., Nguyen, K., Villardi, G. P., Zhao, O., Ishizu, K., & Kojima, F. (2018). Big data analytics, machine learning, and artificial intelligence in next-generation wireless networks. *IEEE access*, *6*, 32328–32338.

Kim, N.-H., An, D., & Choi, J.-H. (2017). Prognostics and health management of engineering systems. *Switzerland: Springer International Publishing*.

Lee, J., Ardakani, H. D., Yang, S., & Bagheri, B. (2015). Industrial big data analytics and cyber-physical systems for future maintenance & service innovation. *Procedia cirp*, *38*, 3–7.

Lee, J., Wu, F., Zhao, W., Ghaffari, M., Liao, L., & Siegel, D. (2014). Prognostics and health management design for rotary machinery systems—reviews, methodology and applications. *Mechanical systems and signal processing*, *42*(1-2), 314–334.

Liu, L., Wang, S., Liu, D., Zhang, Y., & Peng, Y. (2015). Entropy-based sensor selection for condition monitoring and prognostics of aircraft engine. *Microelectronics Reliability*, *55*(9-10), 2092–2096.

Lo, N. G., Soualhi, A., Frinì, M., & Razik, H. (2018). Gear and bearings fault detection using motor current signature analysis. In *2018 13th ieee conference on industrial electronics and applications (iciea)* (pp. 900–905).

Magnus, K., & Jing. (2019). Vibration-based condition monitoring of heavy duty machine driveline parts: Torque converter, gearbox, axles and bearings. *International Journal of Prognostics and Health Management*, *10*(2).

Nectoux, P., Gouriveau, R., Medjaher, K., Ramasso, E., Chebel-Morello, B., Zerhouni, N., & Varnier, C. (2012, June). PRONOSTIA : An experimental platform for bearings accelerated degradation tests. In *IEEE International Conference on Prognostics and Health Management, PHM'12*. (Vol. sur CD ROM, pp. 1–8). Denver, Colorado, United States: IEEE Catalog Number : CPF12PHM-CDR.

Nguyen, K. T. P., Medjaher, K., & Tran, D. T. (2022, September). A review of artificial intelligence methods for engineering prognostics and health management with implementation guidelines. *Artificial Intelligence Review*. doi: 10.1007/s10462-022-10260-y

Omri, N., Al Masry, Z., Mairot, N., Giampiccolo, S., & Zerhouni, N. (2021). Towards an adapted phm approach: Data quality requirements methodology for fault detection applications. *Computers in industry*, *127*, 103414.

Ondel, O., Blanco, E., & Clerc, G. (2007). Beyond the diagnosis: the forecast of state system application in an induction machine. In *2007 ieee international symposium on*

diagnostics for electric machines, power electronics and drives (pp. 491–496).

Ondel, O., Boutleux, E., & Clerc, G. (2005). Adaptive diagnosis by pattern recognition: Application on an induction machine. In *2005 5th ieee international symposium on diagnostics for electric machines, power electronics and drives* (pp. 1–7).

Ooijevaar, T., Pichler, K., Di, Y., & Hesch, C. (2019). A comparison of vibration based bearing fault diagnostic methods. *International Journal of Prognostics and Health Management*, *10*(2).

Ramasso, E., & Saxena, A. (2014). Performance benchmarking and analysis of prognostic methods for cmapss datasets. *International Journal of Prognostics and Health Management*, *5*(2), 1–15.

Sant'Ana, W. C., Lambert-Torres, G., da Silva, L. E. B., Bonaldi, E. L., de Oliveira, L. E. d. L., Salomon, C. P., & da Silva, J. G. B. (2016). Influence of rotor position on the repeatability of frequency response analysis measurements on rotating machines and a statistical approach for more meaningful diagnostics. *Electric Power Systems Research*, *133*, 71–78.

Saxena, A., Celaya, J., Balaban, E., Goebel, K., Saha, B., Saha, S., & Schwabacher, M. (2008). Metrics for evaluating performance of prognostic techniques. In *2008 international conference on prognostics and health management* (p. 1-17). doi: 10.1109/PHM.2008.4711436

Saxena, A., Goebel, K., Simon, D., & Eklund, N. (2008). Damage propagation modeling for aircraft engine run-to-failure simulation. In *2008 international conference on prognostics and health management* (pp. 1–9).

Shi, J., Peng, D., Peng, Z., Zhang, Z., Goebel, K., & Wu, D. (2022). Planetary gearbox fault diagnosis using bidirectional-convolutional lstm networks. *Mechanical Systems and Signal Processing*, *162*, 107996. doi: https://doi.org/10.1016/j.ymssp.2021.107996

Sinha, J. K., & Elbhbah, K. (2013). A future possibility of vibration based condition monitoring of rotating machines. *Mechanical Systems and Signal Processing*, *34*(1-2), 231–240.

Souahli, & Razik. (2020a). *Electrical systems 1. from diagnosis to prognosis*. Wiley-ISTE.

Souahli, & Razik. (2020b). *Electrical systems 2. from diagnosis to prognosis*. Wiley-ISTE.

Soualhi, A., Clerc, G., & Razik, H. (2011). Faults classification of induction machine using an improved ant clustering technique. In *8th ieee symposium on diagnostics for electrical machines, power electronics & drives* (pp. 316–321).

Soualhi, A., Clerc, G., & Razik, H. (2012). Detection and diagnosis of faults in induction motor using an improved artificial ant clustering technique. *IEEE Transactions on Industrial Electronics*, *60*(9), 4053–4062.

Soualhi, A., Medjaher, K., & Zerhouni, N. (2014). Bearing health monitoring based on hilbert–huang transform, support vector machine, and regression. *IEEE Transactions on instrumentation and measurement*, *64*(1), 52–62.

Soualhi, M., Nguyen, K., Medjaher, K., Lebel, D., & Cazaban, D. (2020). Data-driven diagnostics of positioning deviations in multi-axis robots for smart manufacturing. *IFAC-PapersOnLine*, *53*(2), 10330–10335.

Soualhi, M., Nguyen, K. T., & Medjaher, K. (2020). Pattern recognition method of fault diagnostics based on a new health indicator for smart manufacturing. *Mechanical Systems and Signal Processing*, *142*, 106680.

Soualhi, M., Nguyen, K. T., Medjaher, K., Lebel, D., & Cazaban, D. (2022). Intelligent monitoring of multi-axis robots for online diagnostics of unknown arm deviations. *Journal of Intelligent Manufacturing*, 1–17.

Soualhi, M., Nguyen, K. T., Soualhi, A., Medjaher, K., & Hemsas, K. E. (2019). Health monitoring of bearing and gear faults by using a new health indicator extracted from current signals. *Measurement*, *141*, 37–51.

Soualhi, M., Zerhouni, N., Soualhi, A., Hemsas, K., Nguyen, T., & Medjaher, K. (2022). Detection and diagnostics of combined bearing and gear faults using electrical health indicator. In *2022 8th international conference on control, decision and information technologies (codit)* (Vol. 1, pp. 1014–1019).

Strangas, E., Clerc, G., Razik, H., & Soualhi, A. (2021). *Fault diagnosis, prognosis, and reliability for electrical drives*. Wiley-ISTE.

Tamssaouet, F., Nguyen, K. T., Medjaher, K., & Orchard, M. E. (2021). Online joint estimation and prediction for system-level prognostics under component interactions and mission profile effects. *ISA transactions*, *113*, 52–63.

Vachtsevanos, G. J., Lewis, F., Roemer, M., Hess, A., & Wu, B. (2006). *Intelligent fault diagnosis and prognosis for engineering systems* (Vol. 456). Wiley Hoboken.

Wang, D., Tsui, K.-L., & Miao, Q. (2017). Prognostics and health management: A review of vibration based bearing and gear health indicators. *Ieee Access*, *6*, 665–676.

Zarei, J., Tajeddini, M. A., & Karimi, H. R. (2014). Vibration analysis for bearing fault detection and classification using an intelligent filter. *Mechatronics*, *24*(2), 151–157.

Zhang, H., Borghesani, P., Randall, R. B., & Peng, Z. (2022). A benchmark of measurement approaches to track the natural evolution of spall severity in rolling element bearings. *Mechanical Systems and Signal Processing*, *166*, 108466.

Zhang, L., Lin, J., Liu, B., Zhang, Z., Yan, X., & Wei, M. (2019). A review on deep learning applications in prognostics and health management. *Ieee Access*, *7*, 162415–162438.

APPENDIX

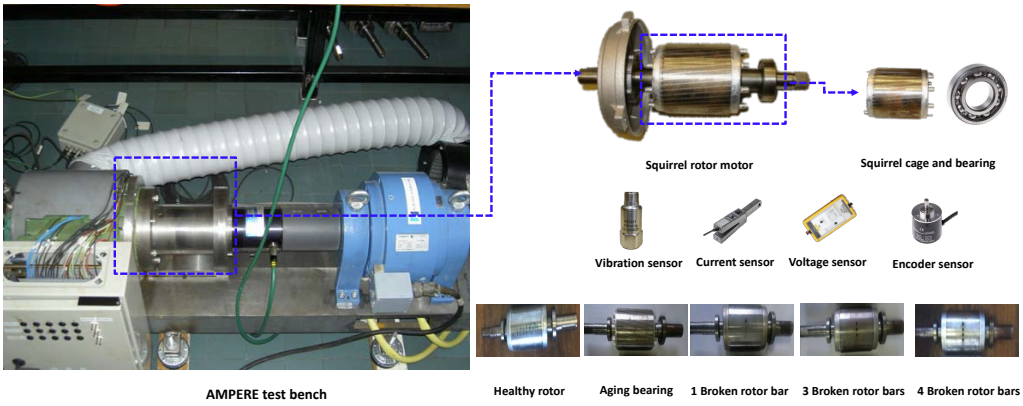

Figure 4. AMPERE test bench for health monitoring of motor rotor faults.

Table 5. Overall view of AMPERE motor rotor experiments.

Monitoring experiments of motor rotor						
System state	Monitoring parameters	Operating conditions		Acquisition parameters		
		Speed (Hz)	Load level (%)	Fs (kHz)	Extension	Time/file (s)
E1: Healthy state	Current, voltage, vibration, speed	24	0, 25, 50, 75, 100	20	.mat, .csv	5
E2: 1 broken bar	Current, voltage, vibration, speed	24	0, 25, 50, 75, 100	20	.mat, .csv	5
E3: 3 broken bars	Current, voltage, vibration, speed	24	0, 25, 50, 75, 100	20	.mat, .csv	5
E4: 4 broken bars	Current, voltage, vibration, speed	24	0, 25, 50, 75, 100	20	.mat, .csv	5
E4: Bearing fault	Current, voltage, vibration, speed	24	0, 25, 50, 75, 100	20	.mat, .csv	5

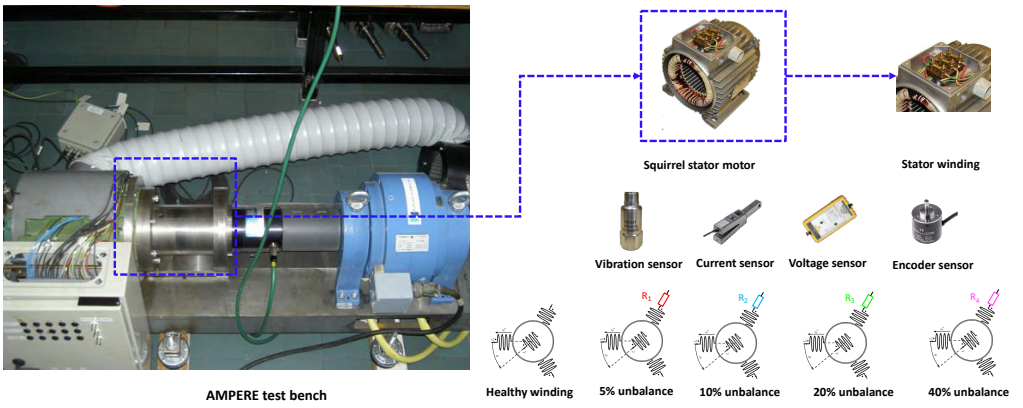

Figure 5. AMPERE test bench for health monitoring of motor stator faults.

Table 6. Overall view of AMPERE motor stator experiments.

Monitoring experiments of motor rotor						
System state	Monitoring parameters	Operating conditions		Acquisition parameters		
		Speed (Hz)	Load level (%)	Fs (kHz)	Extension	Time/file (s)
E1: Healthy state	Current, voltage, vibration, speed	24	0, 25, 50, 75, 100	20	.mat, .csv	5
E2: 05% unbalance	Current, voltage, vibration, speed	24	0, 25, 50, 75, 100	20	.mat, .csv	5
E3: 10% unbalance	Current, voltage, vibration, speed	24	0, 25, 50, 75, 100	20	.mat, .csv	5
E4: 20% unbalance	Current, voltage, vibration, speed	24	0, 25, 50, 75, 100	20	.mat, .csv	5
E5: 40% unbalance	Current, voltage, vibration, speed	24	0, 25, 50, 75, 100	20	.mat, .csv	5

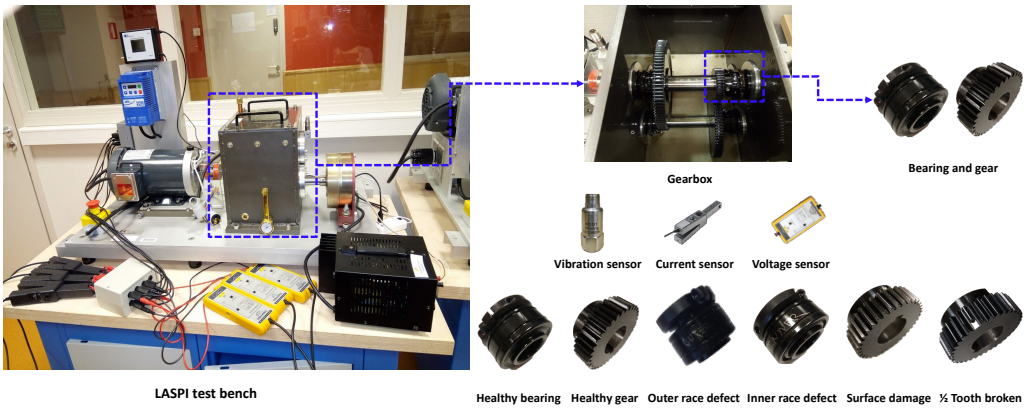

Figure 6. LASPI test bench for health monitoring of bearing and gear components.

Table 7. Overall view of LASPI motor experiments.

Monitoring experiments of gearbox system						
System state	Monitoring parameters	Operating conditions		Acquisition parameters		
		Speed (Hz)	Load level (%)	Fs (kHz)	Extension	Time/file (s)
E1: Healthy state	Current, voltage, vibration	25, 35, 45	0, 25, 50, 75	25.6	.csv	10
E2: Gear surface damage	Current, voltage, vibration	25, 35, 45	0, 25, 50, 75	25.6	.csv	10
E3: Gear 1/2 tooth broken	Current, voltage, vibration	25, 35, 45	0, 25, 50, 75	25.6	.csv	10
E4: Bearing outer ring fault	Current, voltage, vibration	25, 35, 45	0, 25, 50, 75	25.6	.csv	10
E5: Bearing inner ring fault	Current, voltage, vibration	25, 35, 45	0, 25, 50, 75	25.6	.csv	10
E6: E2 & E5	Current, voltage, vibration	25, 35, 45	0, 25, 50, 75	25.6	.csv	10
E7: E3 & E4	Current, voltage, vibration	25, 35, 45	0, 25, 50, 75	25.6	.csv	10

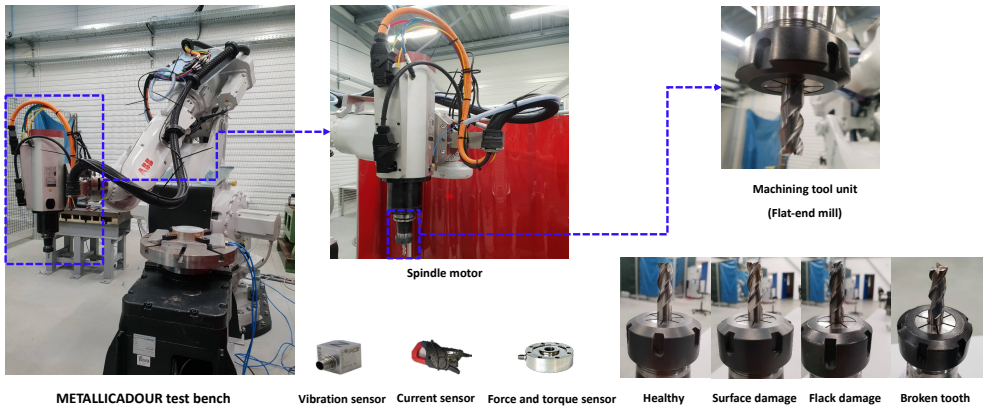

Figure 7. METALLICADOUR test bench for health monitoring of machining tool units.

Table 8. Overall view of METALLICADOUR spindle motor cutting tool experiments.

Monitoring experiments of motor rotor							
System state	Monitoring parameters	Operating conditions			Acquisition parameters		
		Speed (Hz)	Depth (mm)	Feed rate (mm/mn)	Fs (kHz)	File extension	Time/file (s)
E1: Healthy state	Current, vibration, force, torque	233, 300	5, 10	1890, 2730	25.6	.csv	5
E2: Tool surface damage	Current, vibration, force, torque	233, 300	5, 10	1890, 2730	25.6	.csv	5
E3: Tool flack damage	Current, vibration, force, torque	233, 300	5, 10	1890, 2730	25.6	.csv	5
E4: Tool broken tooth	Current, vibration, force, torque	233, 300	5, 10	1890, 2730	25.6	.csv	5

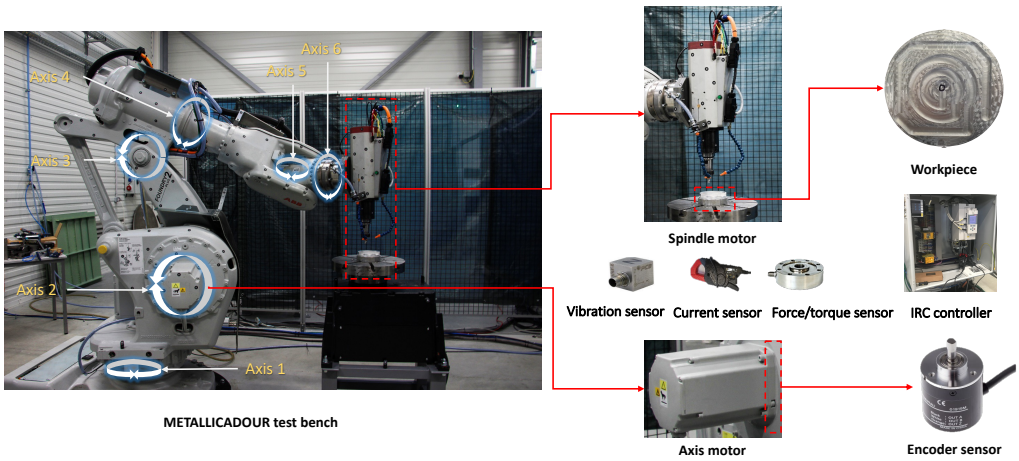

Figure 8. METALLICADOUR test bench for robot axes health monitoring.

Table 9. Overall view of METALLICADOUR axis drifts experiments.

Monitoring experiments of motor rotor									
		Operating conditions				Acquisition parameters			
System state	Monitoring parameters	Speed (Hz)	Depth (mm)	Feed rate (mm/mn)	Degree of drifts (°)	Fs tool (kHz)	Fs axis (Hz)	File extension	Time/file (s)
First group of experiments including unique drifts/axis									
E1: Healthy state 1	Position, current, force, torque, vibration	150	5	648	-	25.6	41.6	.csv .xlsx	5 60
E2: Drifts in axis 1	Position, current, force, torque, vibration	150	5	648	+0.065	25.6	41.6	.csv .xlsx	5 60
E3: Drifts in axis 2	Position, current, force, torque, vibration	150	5	648	+0.120	25.6	41.6	.csv .xlsx	5 60
E4: Drifts in axis 3	Position, current, force, torque, vibration	150	5	648	+0.080	25.6	41.6	.csv .xlsx	5 60
E5: Drifts in axis 4	Position, current, force, torque, vibration	150	5	648	+0.085	25.6	41.6	.csv .xlsx	5 60
E6: Drifts in axis 5	Position, current, force, torque, vibration	150	5	648	+0.120	25.6	41.6	.csv .xlsx	5 60
E7: Drifts in axis 6	Position, current, force, torque, vibration	150	5	648	+0.155	25.6	41.6	.csv .xlsx	5 60
Second group of experiments including combined drifts/axis									
E8: Healthy state 2	Position, current, force, torque, vibration	150	5	648	-	25.6	41.6	.csv .xlsx	5 60
E9: E2 & E5	Position, current, force, torque, vibration	150	5	648	+0.012 -0.04	25.6	41.6	.csv .xlsx	5 60
E10: E3 & E5	Position, current, force, torque, vibration	150	5	648	+0.120 +0.04	25.6	41.6	.csv .xlsx	5 60
E11: E4 & E7	Position, current, force, torque, vibration	150	5	648	-0.04 +0.155	25.6	41.6	.csv .xlsx	5 60
E12: E5 & E6	Position, current, force, torque, vibration	150	5	648	+0.155 -0.04	25.6	41.6	.csv .xlsx	5 60
E13: E6 & E3	Position, current, force, torque, vibration	150	5	648	+0.04 -0.040	25.6	41.6	.csv .xlsx	5 60
E14: E7 & E5	Position, current, force, torque, vibration	150	5	648	+0.18 -0.080	25.6	41.6	.csv .xlsx	5 60

Table 10. Synthesis of published works using the benchmarking data.

Test bench	Paper ID	Studied fault	Data	Condition variation	Objectif	Metric
AMPERE	(M. Soualhi, Nguyen, & Medjaher, 2020)	Motor rotor, motor stator	Current, voltage, vibration	Load level	Detection, diagnostics	Accuracy
	(A. Soualhi et al., 2012)	Motor rotor	Current	Load level	Detection	Error rate
	(Breuneval et al., 2018)	Motor rotor	Current, voltage, vibration	Load level	Detection	Error rate
	(A. Soualhi et al., 2011)	Motor rotor	Current, voltage	Load level	Diagnostics	Error rate
	(Ondel et al., 2007)	Motor rotor	Current, voltage	Load level	Prognostics	-
	(Casimir et al., 2006)	Motor stator	Current, voltage	Load level	Detection, diagnostics	-
	(Ondel et al., 2005)	Motor rotor	Current	Load level	Diagnostics	Error rate
LASPI	(M. Soualhi et al., 2019; M. Soualhi, Zerhouni, et al., 2022)	Bearing, gear, combination of bearing and gear	Current	Load level, speed	Detection, diagnostics	Accuracy
	(M. Soualhi, Nguyen, & Medjaher, 2020)	Bearing, gear, combination of bearing and gear	Current, voltage	Load level, speed	Detection, diagnostics	Accuracy
	(Lo et al., 2018)	Gear	Current	Load level, speed	Detection	-
METALLICADOUR	(M. Soualhi, Nguyen, & Medjaher, 2020)	Robot tool	Current, vibration, force, torque	Depth, speed, feed rate	Detection, diagnostics	Accuracy
	(M. Soualhi, Nguyen, et al., 2022)	Robot axis drifts	Position, current, force, torque, vibration	-	Detection, diagnostics	Accuracy Threshold
	(M. Soualhi, Nguyen, Medjaher, Lebel, & Cazaban, 2020)	Robot axis drifts	Position	-	Diagnostics	-